

## A Linearly Polarized Photon Beam in the CEBAF Hall B

V.B. Ganenko, V.A. Gushchin, Yu.V. Zhebrovsky, L.Ya. Kolesnikov, A.L. Rubashkin,  
and P.V. Sorokin, Kharkov Institute of Physics and Technology

March 12, 1991

## 1. ABSTRACT

We propose to produce a linearly polarized quasimonochromatic photon beam in the CEBAF (Hall B) using the method of coherent bremsstrahlung (CB) of electrons in a single crystal radiator. The employment of such a beam in experiments would provide an important useful tool for studying the dynamics of photonuclear reactions and the structure of particles and nuclei.

## 2. INTRODUCTION

In recent years, considerable interest has been shown to the studies of spin observables in photoprocesses which give information on: nucleon interaction, the structure of few-nucleon systems, the role of meson exchange currents, the contribution of isobar configurations in nuclei, quark degrees of freedom, etc.

Of importance in these studies are the spin parameter measurements of the processes using polarized photon beams and polarized targets, and also the analysis of polarization of reaction products. Presently, polarized photon beams at intermediate energies are planned to be produced practically at all electron accelerators. A similar beam is proposed to be produced at CEBAF (Hall B).

The analysis of the existing methods of linearly polarized photon beam generation (CB [1], off-axis tagged photon collimation of the bremsstrahlung [2], backward Compton scattering of light on a fast electron [3]), has shown the first two methods to be most promising for the CEBAF (Hall B). Though in the case of Compton scattering of light nearly a 100% photon polarization can be obtained, the energy and intensity are low.

The CB spectrum is characterized by the presence of a number of quasimonochromatic peaks, whose intensity and position depend on the structure of a single crystal radiator and its orientation relative to the electron beam. As the relative energy of  $\gamma$ -quanta ( $x = E_\gamma / E_0$ ) grows, the peak intensity and, hence, the degree of linear polarization in radiation peaks decrease, therefore, it appears most efficient to use this method in the energy range  $0.1' \leq x \leq 0.5$ . The photon polarization from a diamond single crystal changes in this case from 0.9 down to 0.4 and then becomes practically zero.

With the off-axis tagged photon beam the polarization value can exceed 0.7 at low photon energies and still be  $\approx 0.2$

at  $x \approx 0.8$ . Even though this method is more labour consuming because of strict requirements to the accuracy in installation of the radiator, the collimator, the residual-electron detector, it seems to us reasonable to develop at CEBAF both techniques of polarized photon beam production, which would complement each other nicely in the whole energy range.

Work at producing and investigating a CB beam at the Kharkov 2 GeV electron linac has been carried out since 1966. We have developed various methods of single crystal radiator orientation [4,5], determination of the degree of polarization at the peak of radiation using the coherent effect [6,7]. The polarized photon beam has been employed to investigate spin observables in the processes of meson photoproduction on nucleons and photodisintegration of lightest nuclei, both in single- and double- polarization experiments by the use of polarized targets and recoil-nucleon polarization measurements [8-11]. Thus, the experience acquired during this work can efficiently be used for production and operation of the CB beam in the CEBAF (Hall B).

### 3. EXPERIMENTAL EQUIPMENT

Practically all experimental equipment which has been installed in the Hall B in order to produce a tagged photon beam can also be used to produce a CB beam. The main additional units of the equipment will be a goniometer device with a single crystal radiator, and a soft - photon detection system ( e.g., a thin-walled ionization chamber) intended to choose single-crystal orientation relative to the electron beam.

The proposed layout of the experimental equipment is shown in Fig.1. The goniometer with a single crystal is placed at approximately 3 m ahead of the tagging magnet. The required photon-beam and collimation-angle sizes are ensured by an adjustable collimator installed together with a cleaning magnet in front of the CLAS. Behind the detector there is a

thin-walled ionization chamber, which is used for orientation of the single-crystal radiator.

### 3.1. GONIOMETER

The goniometer device is intended for orientation of a single-crystal radiator relative to the primary electron momentum  $P_0$ . Coherent effects take place in the case when the chosen axis  $b_1$  of the single crystal makes a small angle  $\theta$  with the momentum  $P_0$ , and the azimuthal angle  $\alpha$  is determined by the  $(P_0, b_1)$  and  $(b_1, b_2)$  planes. The scheme of the goniometer is shown in Fig.2 [12]. The device is a set of frames 5, 10 through which the single crystal 1 rotates around mutually perpendicular horizontal ( $f_H$ ) and vertical ( $f_V$ ) axes, and also around the azimuthal axis  $f_A$  normal to  $f_H$ . The angles of goniometer rotation are related to the angles of single-crystal orientation  $\theta$  and  $\alpha$  as

$$\Phi_V = \Phi_V^0 + \theta \cos(\alpha + \varphi)$$

$$\Phi_H = \Phi_H^0 + \theta \sin(\alpha + \varphi)$$

$$\Phi_A = \Phi_A^0 + \varphi ,$$

where  $\Phi_V^0$ ,  $\Phi_H^0$  are the initial orientation angles, at which the crystal axis  $b_1$  is parallel to the momentum  $P_0$ ,  $\varphi$  is the angle between the axes  $b_2$  ( $b_3$ ) and  $f_V$  ( $f_H$ ).

At our Institute, we have constructed the goniometer with the parameters listed in Table 1.

### 3.2. A SINGLE CRYSTAL TARGET

The CB beam parameters substantially depend on the single crystal type. Here the most important characteristics are the density of atomic packing, Debye temperature and the

manufacturability. The analysis of these properties among different crystals has led one to choose diamond, silicon and beryllium as radiators (see Table 2). As it follows from the estimates given below, diamond provides the highest coherent effect and, hence, the highest degree of polarization. In its turn, silicon is easily adaptable to produce rather thin samples, and this is essential for CB beam monochromatization [13]. In this respect, a single crystal of beryllium appears rather promising. Yet, in this case there are some problems with preparing samples larger than 2 or 3 mm without any substantial defects of the structure.

Since in Hall B there is no necessity for high photon beam intensities, the main requirement in choosing the single-crystal radiator thickness should be the possibility of attaining the highest degree of polarization and the monochromaticity of the photon beam. The method of tight collimation of photons is most effective in the case where the angle of multiple scattering in the radiator is smaller than the natural emission angle  $mc^2/E_0$ . In view of this criterion, the crystal thickness should not exceed 0.1 mm ( $7.5 \times 10^{-4}$  rad.length) and 0.07 mm for diamond and silicon, respectively. The multiple-scattering angle for these thickness values at initial electron energies of 4 GeV is equal to  $\approx 10^{-4}$  rad.

### 3.3. DETERMINATION OF SINGLE CRYSTAL ORIENTATION

As mentioned above, the CB intensity and polarization spectra essentially depend on the single crystal orientation angles  $\theta$  and  $\alpha$  with respect to the initial electron momentum  $P_0$ . For  $\theta \ll 1$  and  $\alpha = 0^\circ$  (or  $\pi/2$ ), the cross section for the CB is contributed by a row of reciprocal lattice points of the single crystal ("the effect of the row").

Even though the intensity at the CB peak is high, the polarization degree is not large in this case, because the contributions from different lattice points of the row may suppress each other. For  $0 < \alpha < \pi/2$  one can choose such a

target orientation, at which the contribution to the CB cross section comes from a single reciprocal lattice point ( "the effect of the point" ). In this case, the polarization is maximum. Since there is no special need for high intensities in Hall B, the last-mentioned type of orientation is preferable.

Below we consider the methods of determining the initial single crystal orientation ( $\theta=0$ ,  $\alpha=0$ ). To solve this problem, we use the dependence of the CB cross section on crystal orientation angles [4,14]. The most pronounced dependences are observed in the case of low-energy photon detection [14] (Fig.3). The initial single crystal orientation is determined by constructing a map of discrete CB peaks resulting from particular points of the diamond reciprocal lattice in the  $\Phi_V$  -  $\Phi_H$  coordinates of the angles of goniometer rotation. Using the Kharkov 2 GeV electron linac facilities, we have measured the number of low energy photons  $N_\gamma$  as a function of the rotation angle  $\Phi_H$  for three fixed arbitrarily chosen angles of the goniometer rotation  $\Phi_V = 60, 50$  and  $40$  mrad (see curves 3a, b, c, respectively). The orientation angles  $\Phi_V^0$ ,  $\Phi_H^0$  were calculated by solving the set of equations of the intersecting straight lines passing through the coordinates of the discrete peaks from the lattice points with the like Miller indices (Fig.3d). The map inclination is due to the lack of coincidence between the crystal axes  $b_2$ ,  $b_3$  and the corresponding axes of goniometer rotation  $f_V$ ,  $f_H$  (in our example,  $\varphi = 13^\circ 18'$ ). These axes were aligned by rotating the crystal around the axis  $f_A$  by the angle  $\varphi$ , and as is seen from Fig.3e, the orientational dependence becomes symmetric with respect to the peak from the "strongest" ( $2\bar{2}0$ ) point of the diamond crystal reciprocal lattice.

### 3.4. CB INTENSITY AND POLARIZATION SPECTRA

Figures 4 to 7 show the calculated CB intensity and polarization spectra from diamond and silicon single-crystals

with thicknesses 0.1 and 0.07 mm, respectively, for CEBAF energies. The spectra were calculated both for no photon beam collimation on the physical target, and for the collimation angle  $\theta_c = 0.5$  (in the units of the natural photon emission angle  $mc^2/E_0$  for the  $(2\bar{2}0)$  point orientation. The CB beam parameters estimated from these spectra are given in Table 3, from which it can be seen that the highest polarization degree and the beam merit factor are attained in the case of the collimation angle  $\theta_c = 0.5$  of the radiation from a thin diamond single crystal. Rather high polarization degree and beam monochromaticity also take place in the case of a silicon single crystal from which, as mentioned above, it is easier to prepare thin single crystal plates.

### 3.5. CONTROL OF THE PHOTON POLARIZATION DEGREE

During the measurements of spin observables the CB parameters may change. To control the beam polarization degree, one can employ a simple method [6,7], where the correlation between polarization and intensity of the CB is used. For an isolated reciprocal lattice point this correlation is given by a simple relationship

$$P_\gamma = k \frac{2(1-x)}{1+(1-x)^2} \frac{\beta - 1}{\beta}$$

where  $k$  is the calculated coefficient taking into account the special features of target orientation and structure,  $\beta$  is the ratio of yields from the process under study in the cases of the oriented and unoriented single-crystal. Another possibility of investigating and controlling the CB beam parameters lies in a continuous measurement of the photon spectrum by the pair spectrometer and in arranging the feedback with the control board, the electron beam and the goniometer [15].

#### 4. CONCLUSION

In the CB production at the CEBAF (Hall B) the Kharkov Institute of Physics and Technology can undertake:

- to make a goniometer device with the parameters given in Table 1;

- to prepare diamond and silicon single crystals ;

- to participate in the CB beam production and in measurements of spin observables.

## REFERENCES

1. G.Diambrini Palazzi, Rev.Mod.Phys., 40, 611 (1968).
2. R.M.Laszewsky, Program at CEBAF (II). Report of the 1986 Summer Study Group, 1986, p.667-673.
3. R.H.Milburn, Phys. Rev. Lett., 10, 75 (1963)
4. V.G.Gorbenko et al., Yad. Fiz., 11, 1044 (1970)
5. V.G.Gorbenko et al., Prib. Tekh. Eksp., N2, 54 (1973)
6. V.G.Gorbenko et al., Yad. Fiz., 17, 793 (1973)
7. L.Ya.Kolesnikov, A.L.Rubashkin, V.M.Sanin, Ukr.Fiz.Zh., 29, 1296 (1984)
8. A.S.Bratashevsky et al., Nucl. Phys., B166, 525 (1980)
9. V.A.Get'man et al., Nucl. Phys., B188, 397 (1981)
10. V.G.Gorbenko et al., Nucl. Phys., A381, 330 (1982)
11. A.A.Belyaev et al., Nucl. Phys., B213, 201 (1983)
12. N.A.Agarkov et al., Prib. Tekh. Eksp., N2, 57 (1979)
13. R.F.Mozley, J.de Wire, Nuovo Cim., 27, 1281 (1963)
14. D.Luckey, R.F.Schwitters, Nucl. Instr. and Meth., 81, 164(1970)
15. A.Jackson, Nucl. Instr. and Meth., 129, 73 (1975)

TABLE 1. PERFORMANCE CHARACTERISTICS OF THE KIPT GONIOMETER.

Range of rotation around the axes:	
vertical .....	$\pm 8^\circ$
horizontal .....	$\pm 8^\circ$
azimuthal .....	$0^\circ \dots 360^\circ$
Angle of frame rotation per motor step	
vertical and horizontal axes .....	$1 \times 10^{-5}$ rad
azimuthal axis .....	$2.5 \times 10^{-3}$ rad

TABLE 2. MAIN PARAMETERS OF THE SINGLE CRYSTAL EMPLOYED  
FOR CB BEAM PRODUCTION

Parameter	Single crystal		
	Diamond	Silicon	Beryllium
Atomic number	6	14	4
Atomic weight	12	28	9
Density, g/cm <sup>3</sup>	3.51	2.4	1.84
Lattice type	diamond	diamond	hexagonal
Lattice constant, Å	3.568	5.431	a <sub>1</sub> =a <sub>2</sub> =0.364 a <sub>3</sub> =0.571
Debye temperature, K	1850	650	—
Debye factor	127	270	412
Radiation length, g/cm <sup>2</sup>	43.3	22.2	63.7

TABLE 3. EXPECTED CB BEAM PARAMETERS IN THE CEBAF (Hall B)  
AT AN INITIAL ENERGY  $E_0 = 4$  GeV.

Parameters	Diamond		Silicon	
	$\theta_c = \infty$	$\theta_c = 0.5$	$\theta_c = \infty$	$\theta_c = 0.5$
Number of photons $dN_\gamma/dE_\gamma$ ( $\text{GeV}^{-1} \cdot \mu\text{A}^{-1}$ )				
$E_\gamma^{\text{peak}} = 1$ GeV	$10^{10}$	$7.5 \times 10^9$	$2 \times 10^9$	$1.1 \times 10^9$
$E_\gamma^{\text{peak}} = 2$ GeV	$1.8 \times 10^9$	$10^9$	$5.9 \times 10^8$	$2.2 \times 10^8$
Monochromaticity, $\Delta E_\gamma/E_\gamma$				
$E_\gamma^{\text{peak}} = 1$ GeV	0.35	0.2	0.35	0.15
$E_\gamma^{\text{peak}} = 2$ GeV	0.3	0.125	0.3	0.1
Polarization, $P_\gamma$				
$E_\gamma^{\text{peak}} = 1$ GeV	0.71	0.88	0.45	0.77
$E_\gamma^{\text{peak}} = 2$ GeV	0.42	0.65	0.2	0.48
Merit factor, $I \cdot P_\gamma^2$				
$E_\gamma^{\text{peak}} = 1$ GeV	5.545	5.94	0.405	0.652
$E_\gamma^{\text{peak}} = 2$ GeV	0.623	0.845	0.051	0.103

## FIGURE CAPTIONS

- FIG.1. Layout of the experimental equipment in Hall B.
- FIG.2. Diagram of the goniometer  
1: single crystal target; 2: sliding carriage;  
3,7,9: step motor; 4: crystal holder casing;  
5(10): inner (outer) frame; 6,8: pushers; 11: support.
- FIG.3. Procedure of determining the diamond single crystal orientation: a, b, c: orientational dependences of the number of low energy photons at  $\Phi_V=60, 50$  and  $40$  mrad. d: map of discrete peaks in the  $\Phi_V - \Phi_H$  coordinates; e: the same as in Fig.3 c, but for  $\phi = 0$ .
- FIG.4. CB intensity (a) and polarization (b) spectra from a diamond single crystal,  $0.1$ mm thick,  $\theta=75$  mrad,  $\alpha=89^\circ 08'$ . The electron beam divergence is  $10^{-4}$  rad. Collimation angle  $\theta_c = \infty$  (solid curve),  $\theta_c = 0.5$  (dashed curve)
- FIG.5. The same as in FIG.4, but for  $\alpha=87^\circ 25'$ .
- FIG.6. CB intensity (a) and polarization (b) spectra from a silicon single crystal,  $0.07$  mm thick,  $\theta=75$  mrad,  $\alpha=88^\circ 6'$ . The remaining parameters are the same as those in FIG.4.
- FIG.7. The same as in FIG.6, but for  $\alpha=85^\circ 32'$ .

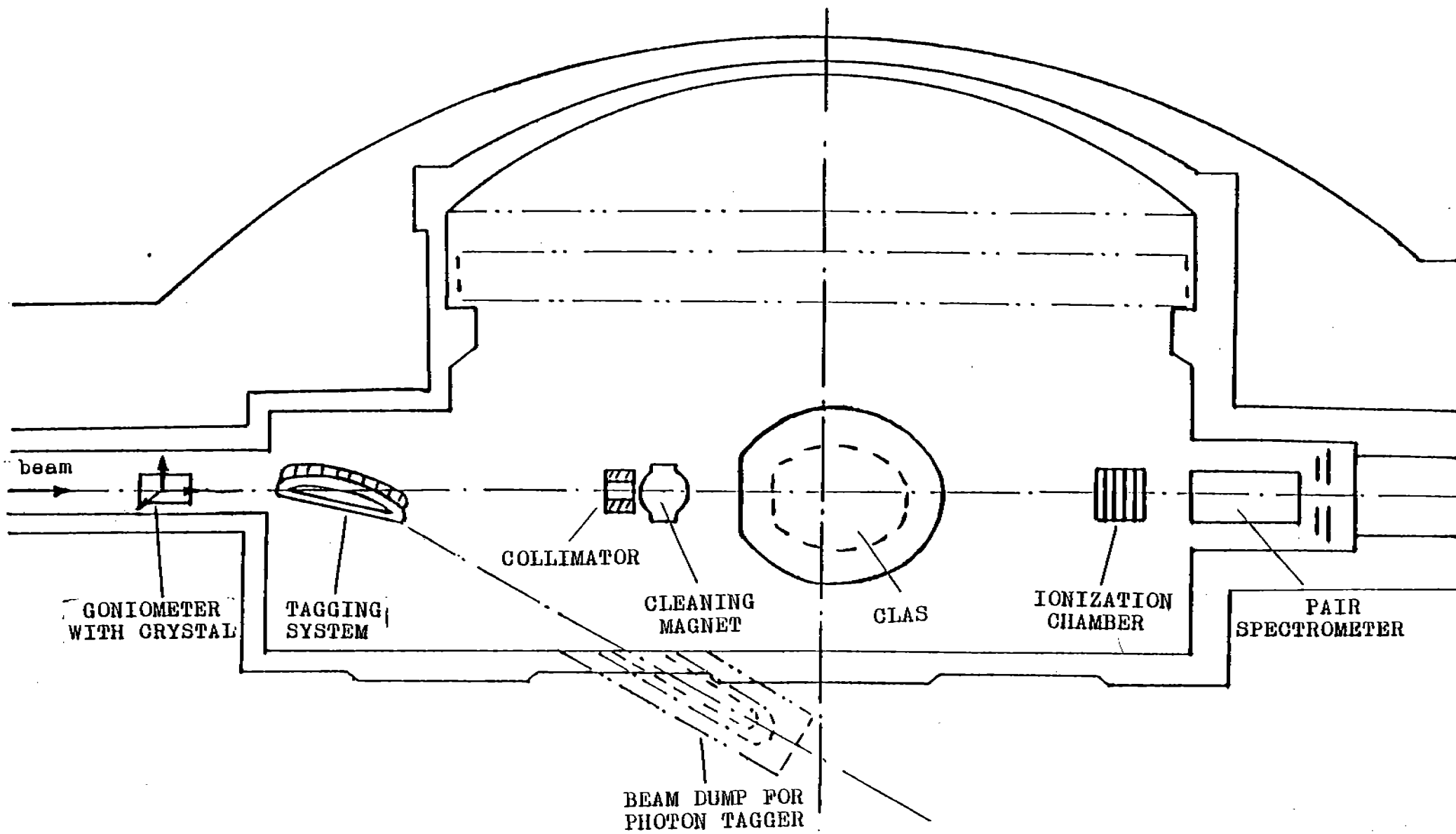


FIG.1. LAYOUT OF THE EXPERIMENTAL EQUIPMENT IN HALL B.

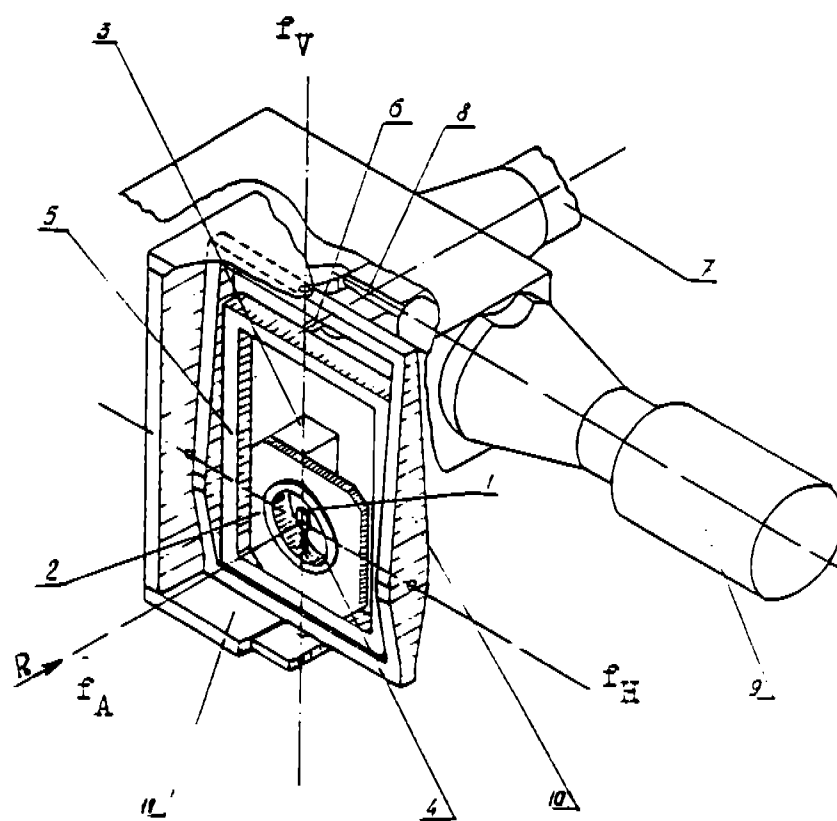


FIG.2. DIAGRAM OF THE GONIOMETER

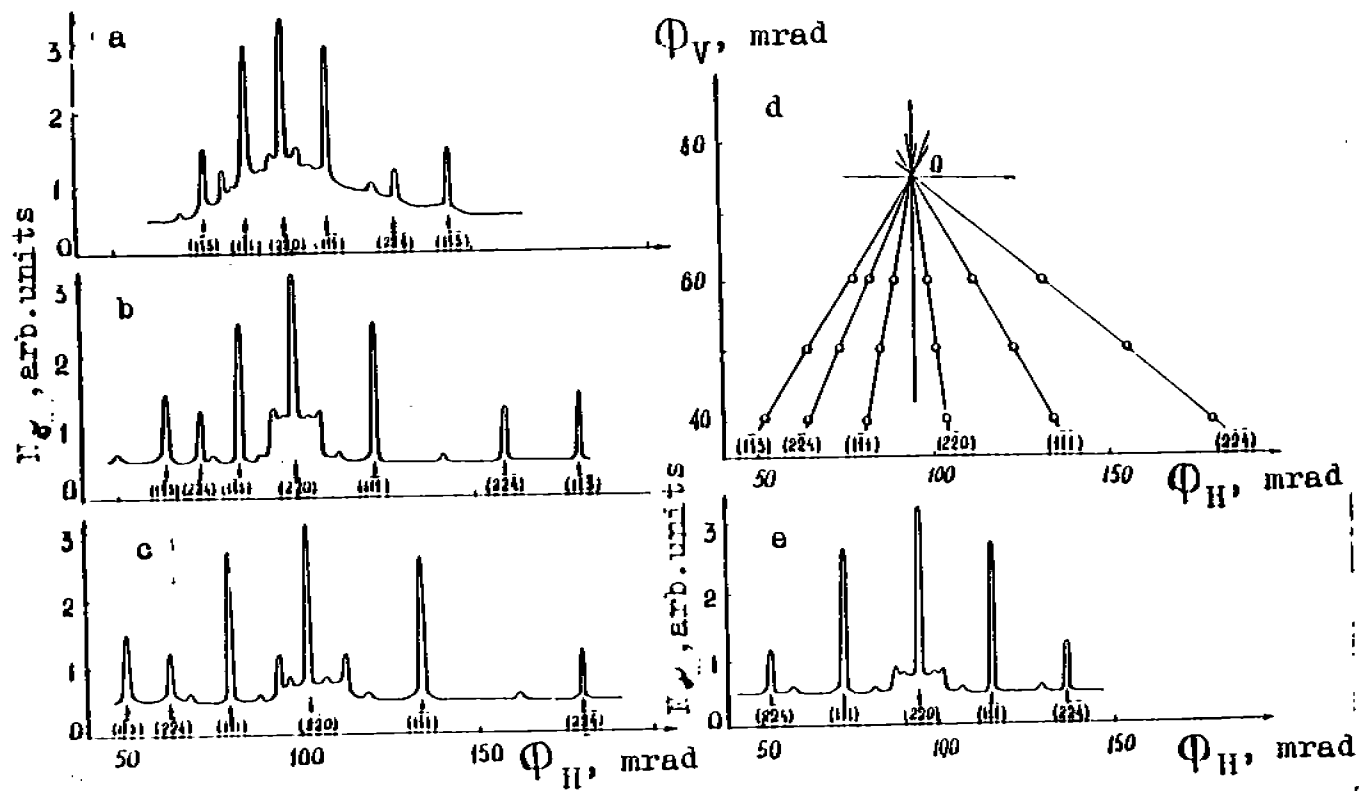


FIG. 3. PROCEDURE OF DETERMINING THE DIAMOND SINGLE CRYSTAL ORIENTATION.

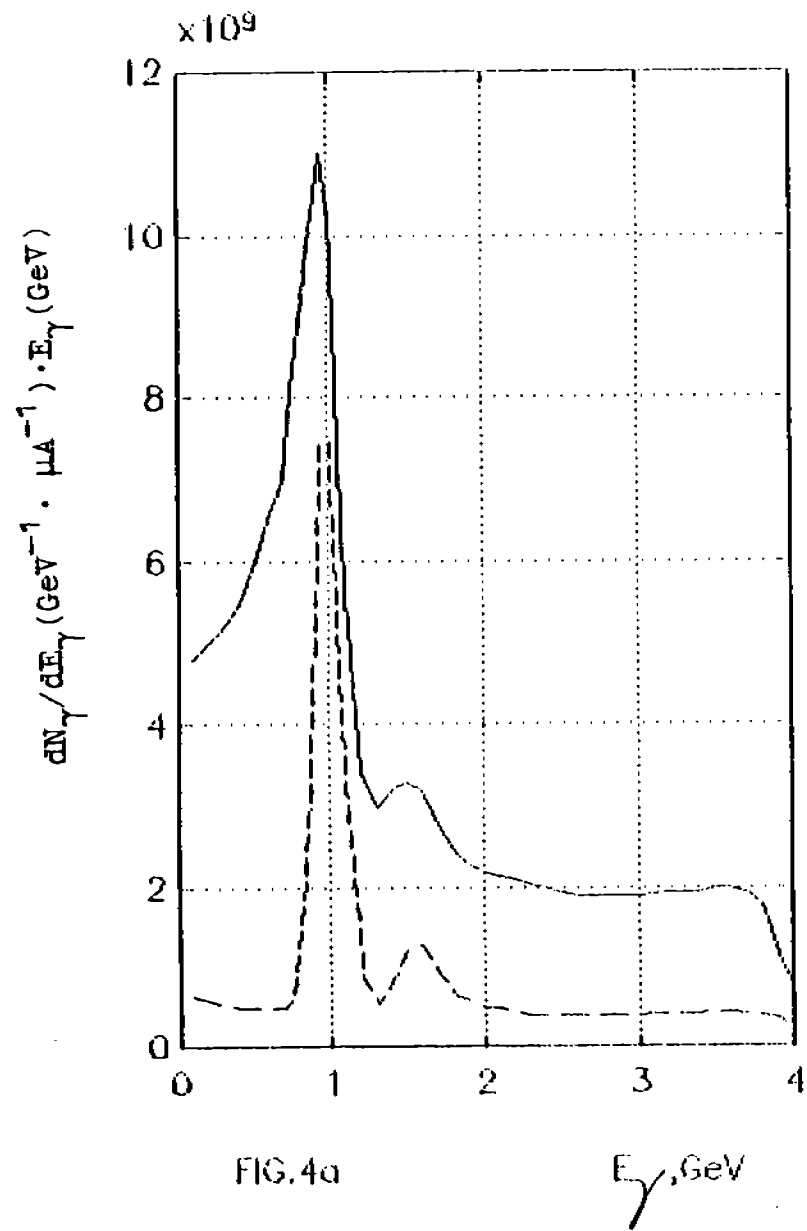


FIG. 4a

$E_\gamma, \text{GeV}$

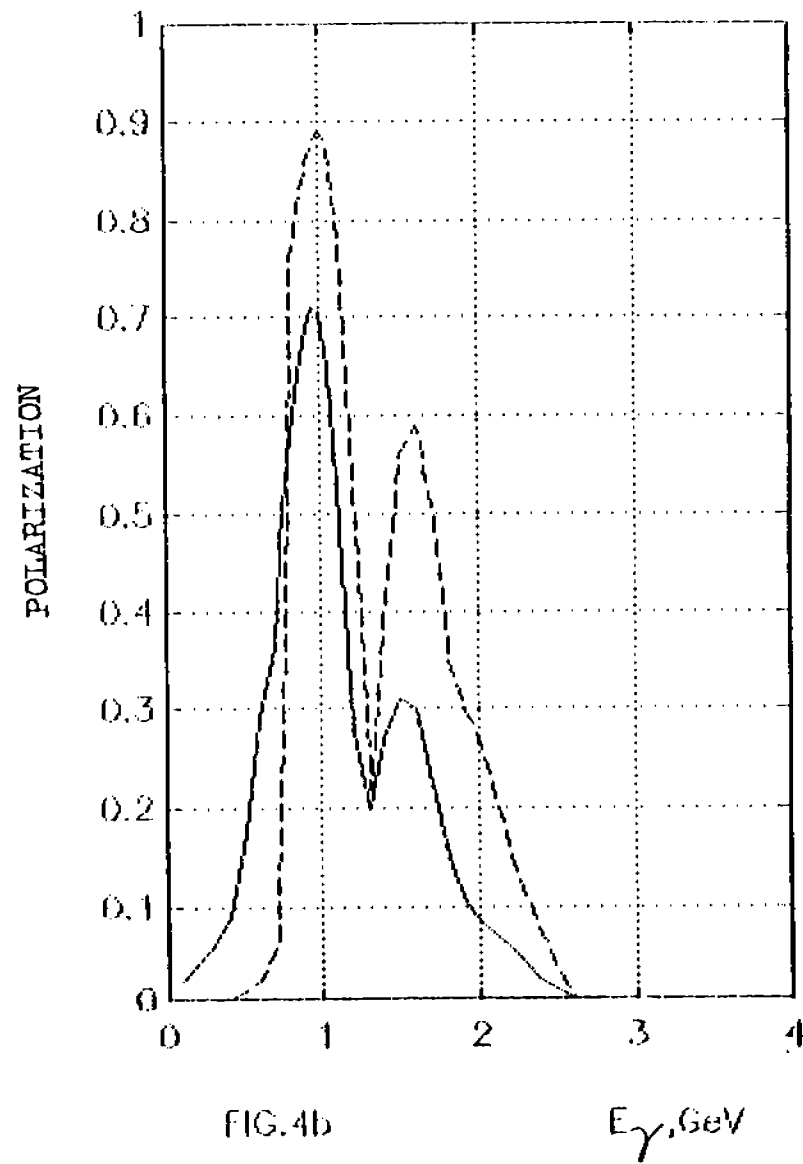
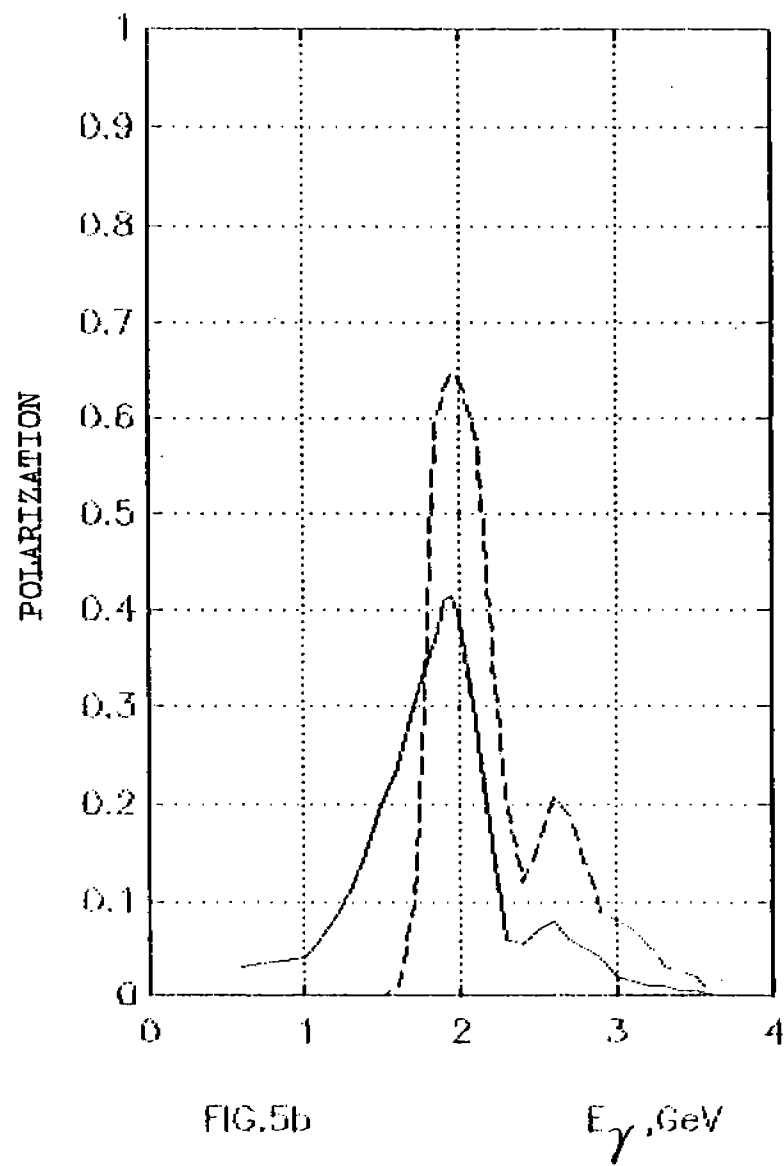
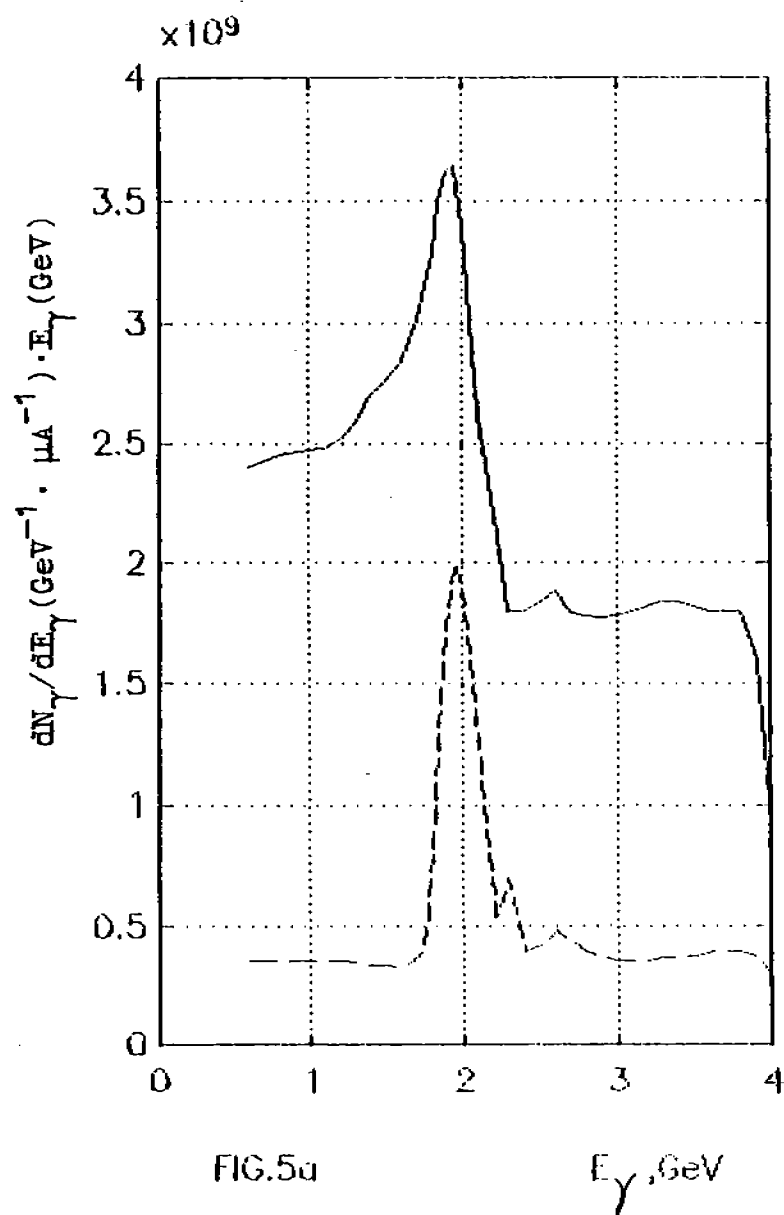
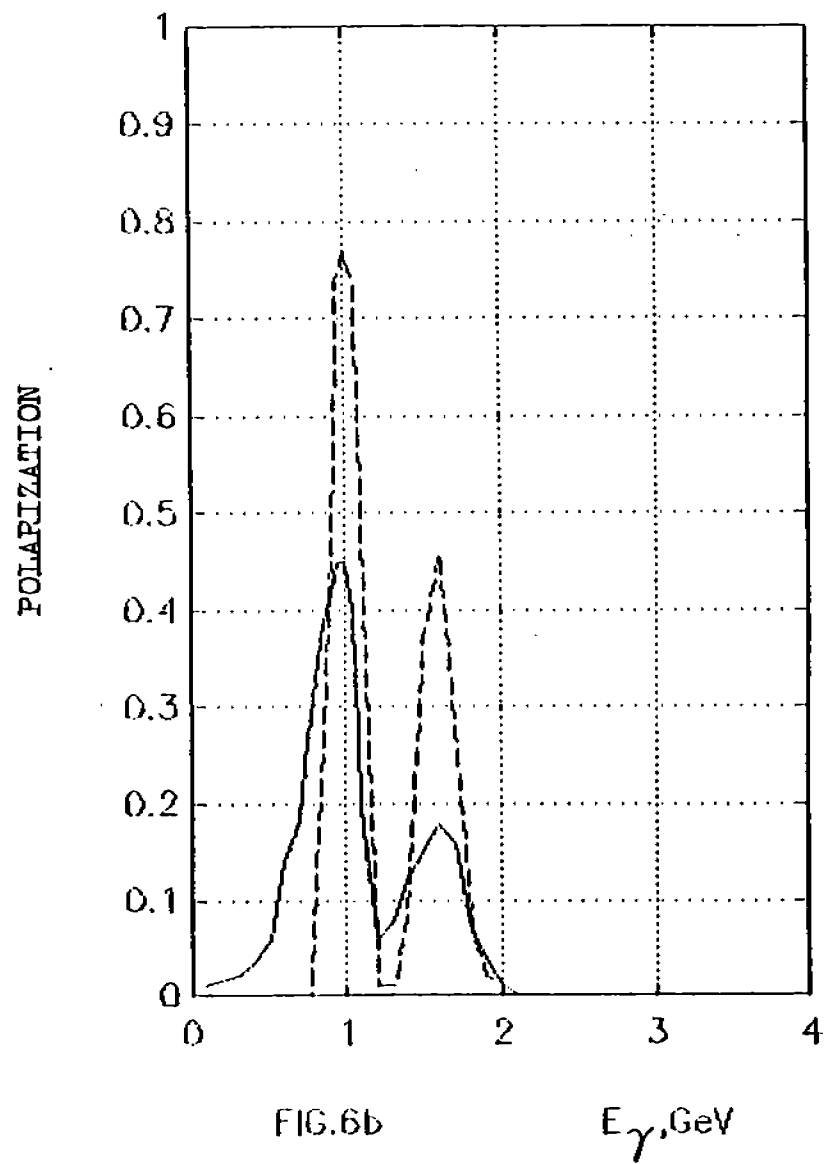
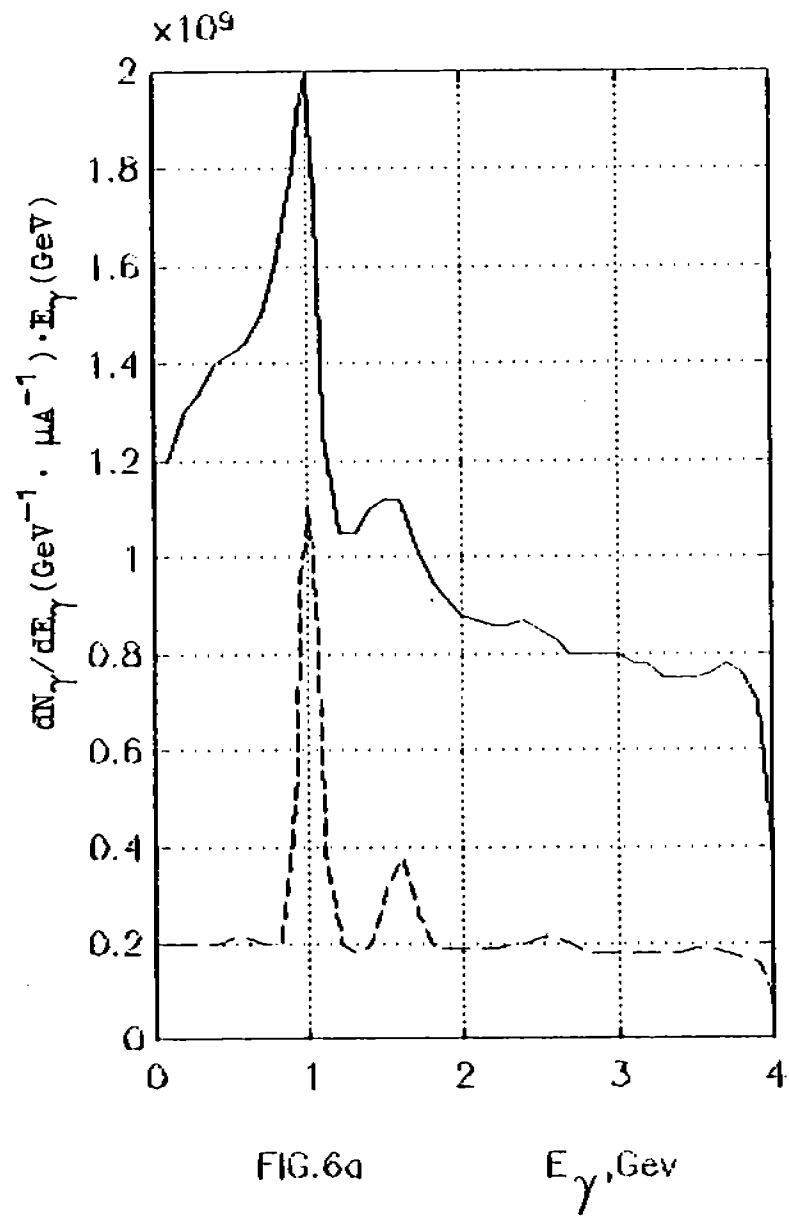


FIG. 4b

$E_\gamma, \text{GeV}$





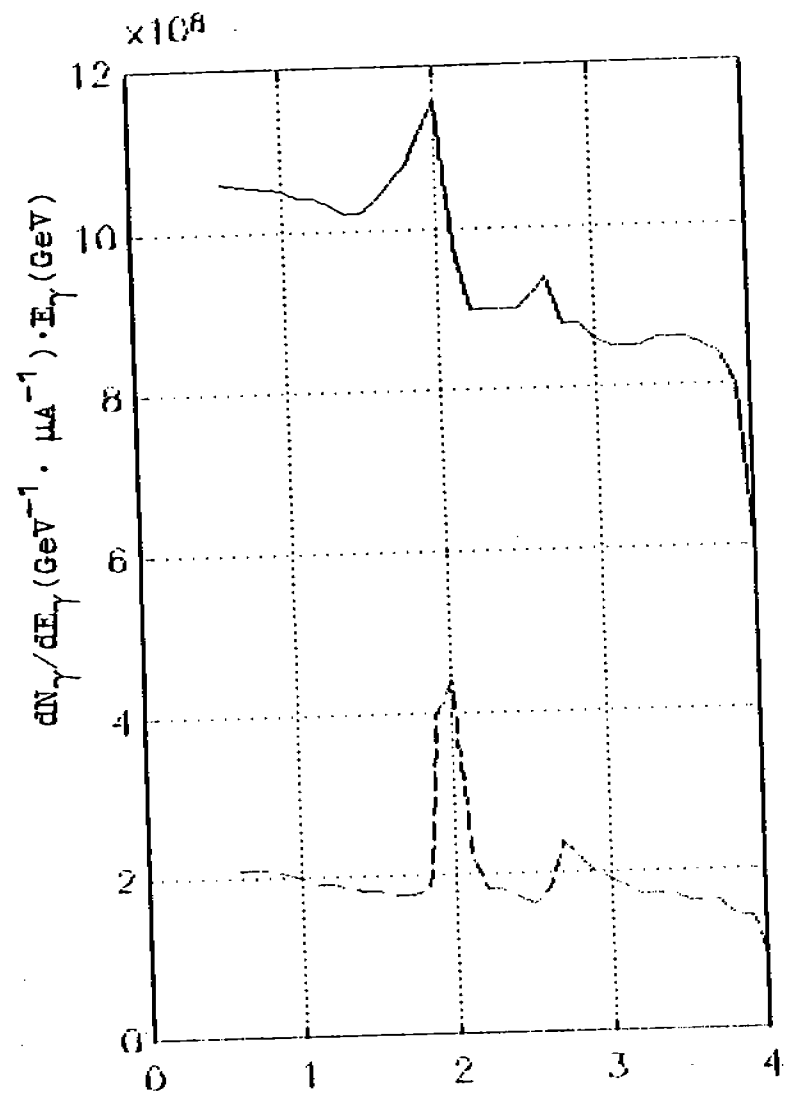


FIG. 7a

$E_\gamma$ , GeV

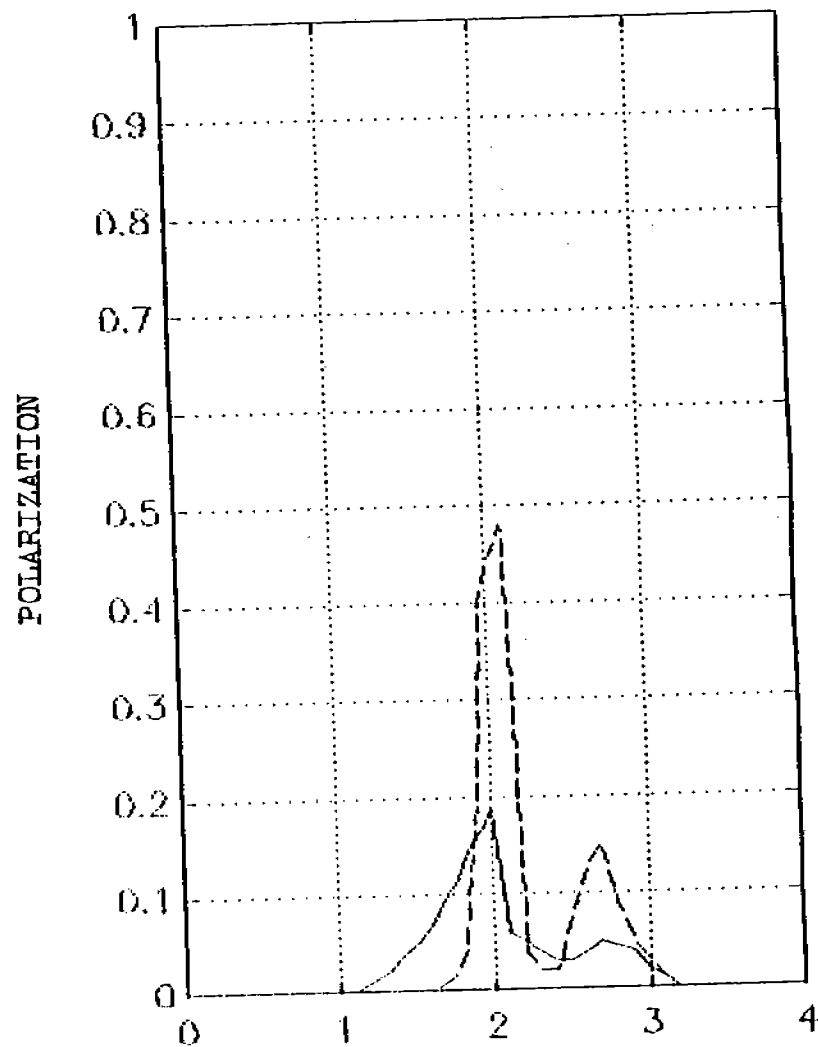


FIG. 7b

$E_\gamma$ , GeV